

*Communication*

## Gas-Foamed Scaffold Gradients for Combinatorial Screening in 3D

Kaushik Chatterjee<sup>1,2</sup>, Alison M. Kraigsley<sup>1</sup>, Durgadas Bolikal<sup>3</sup>, Joachim Kohn<sup>3</sup> and Carl G. Simon Jr.<sup>1,\*</sup>

<sup>1</sup> Polymers Division, National Institute of Standards & Technology, 100 Bureau Drive, Gaithersburg, MD 20899, USA; E-Mail: alison.kraigsley@nist.gov

<sup>2</sup> Department of Materials Engineering, Indian Institute of Science, Bangalore 560012, India; E-Mail: kchatterjee@materials.iisc.ernet.in

<sup>3</sup> New Jersey Center for Biomaterials, Rutgers University, Piscataway, NJ 08854, USA; E-Mails: bolikal@biology.rutgers.edu (D.B.); kohn@rutgers.edu (J.K.)

\* Author to whom correspondence should be addressed; E-Mail: carl.simon@nist.gov; Tel.: +1-301-975-8574; Fax: +1-301-975-4977.

*Received: 6 February 2012; in revised form: 28 February 2012 / Accepted: 1 March 2012 / Published: 7 March 2012*

---

**Abstract:** Current methods for screening cell-material interactions typically utilize a two-dimensional (2D) culture format where cells are cultured on flat surfaces. However, there is a need for combinatorial and high-throughput screening methods to systematically screen cell-biomaterial interactions in three-dimensional (3D) tissue scaffolds for tissue engineering. Previously, we developed a two-syringe pump approach for making 3D scaffold gradients for use in combinatorial screening of salt-leached scaffolds. Herein, we demonstrate that the two-syringe pump approach can also be used to create scaffold gradients using a gas-foaming approach. Macroporous foams prepared by a gas-foaming technique are commonly used for fabrication of tissue engineering scaffolds due to their high interconnectivity and good mechanical properties. Gas-foamed scaffold gradient libraries were fabricated from two biodegradable tyrosine-derived polycarbonates: poly(desaminotyrosyl-tyrosine ethyl ester carbonate) (pDTEc) and poly(desaminotyrosyl-tyrosine octyl ester carbonate) (pDTOc). The composition of the libraries was assessed with Fourier transform infrared spectroscopy (FTIR) and showed that pDTEc/pDTOc gas-foamed scaffold gradients could be repeatably fabricated. Scanning electron microscopy showed that scaffold morphology was similar between the pDTEc-rich ends

and the pDTOc-rich ends of the gradient. These results introduce a method for fabricating gas-foamed polymer scaffold gradients that can be used for combinatorial screening of cell-material interactions in 3D.

**Keywords:** combinatorial screening; polymer; scaffold; tissue engineering

---

## 1. Introduction

Combinatorial and high-throughput technologies are being applied for discovery in tissue engineering research to systematically screen cell-biomaterial interactions [1,2]. In current methods, material surfaces are prepared either as a continuous gradient or an array library where a property of the biomaterial is systematically varied [3–7]. Cells are seeded on the biomaterial libraries and optimal properties are determined through measurement of the desired cellular responses. For example, cell response to polymer blends was measured using gradient scaffolds prepared from poly( $\epsilon$ -caprolactone) (PCL) and poly(D,L)lactic acid (PDLLA) to identify an optimal composition for osteoblast proliferation and differentiation [3]. A large library of photopolymerized materials was screened using high-throughput technology to identify optimal substrates to support human embryonic stem cells in feeder-free conditions [6]. Orthogonal gradients in surface wettability and topography were fabricated to screen osteoblast response to biomaterial surface properties [5]. A combination of array and gradient approaches was applied to screen cell response to composition of dental composites [4]. In another study, “topochips” were designed to rapidly screen the effect of surface topography on mesenchymal stem cell proliferation and differentiation [7].

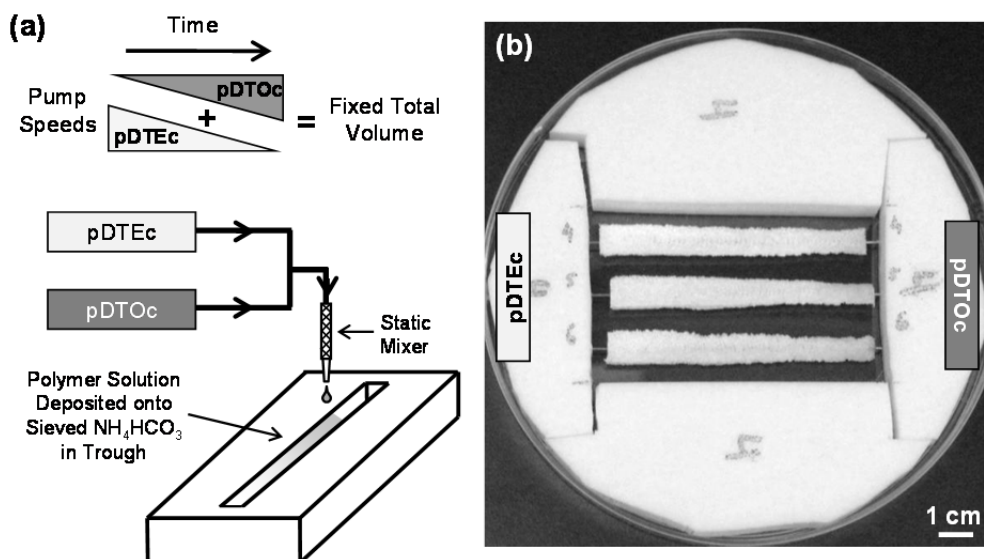
However, in tissue engineering, biomaterials are commonly processed into three-dimensional (3D) scaffold for tissue regeneration [8]. Cells are sensitive to topographical differences between 2D surfaces and 3D scaffolds [9,10] and studies indicate that cell response in 3D scaffolds is more representative of *in vivo* behavior than that observed in a 2D culture format [11–13]. Thus, there is a need to design combinatorial techniques to screen 3D tissue scaffolds. A few recent studies have utilized combinatorial 3D tissue scaffolds [14–18]. For example, gradient hydrogels were fabricated to screen the effect of 3D scaffold modulus on encapsulated osteoblasts [15]. Arrays of salt-leached macro-porous scaffolds were prepared to measure osteoblast response to polymer blend composition [14]. In other work, gradient and array library formats were compared for assessing osteoblast response to the mass fraction of amorphous calcium phosphate included in 3D composite salt-leached scaffolds [18]. Finally, the effect of different extracellular matrix proteins on embryonic stem cell differentiation was studied using combinatorial hydrogel scaffold libraries [17].

In the current work, we aimed to develop an approach for fabricating gas-foamed scaffold gradients that can be used for combinatorial screening in 3D. Previously, we developed a two-syringe pump approach for fabricating salt-leached scaffold gradients [14,18–20]. However, gas-foamed scaffolds have several advantages over salt-leached scaffolds. Gas-foamed scaffolds use gas bubbles to create porous polymer scaffolds [21–24]. The gas-foaming process yields scaffolds with pores that are better connected than those in salt-leached scaffolds and gas-foamed scaffolds also have stronger mechanical properties [21]. Salt-leaching also leaves a polymer skin on scaffolds that can prevent cells from

penetrating the scaffold interior while the gas-foaming process yields a scaffold with uniform pore distribution and no skin [22]. Gas-foamed scaffolds support adhesion, proliferation and differentiation of osteoblasts to yield bone-like tissues [23,24].

A two-syringe pump approach (Figure 1) [18,19] was adapted to fabricate gas-foamed scaffold gradients. In order to demonstrate the feasibility of this approach, blends of two degradable tyrosine polycarbonates, poly(desaminotyrosyl-tyrosine ethyl ester carbonate) (pDTEc) and poly(desaminotyrosyl-tyrosine octyl ester carbonate) (pDTOc), were used to fabricate gas-foamed scaffold libraries. Tyrosine polycarbonates are being advanced for use in implantable biomedical devices such as hernia repair meshes, cardiovascular stents and bone tissue engineering scaffolds [25,26]. pDTEc and pDTOc have the same backbone but different side chains (Figure 2). These different side chains cause differences in the polymer properties including water contact angle ( $71^\circ$  for pDTEc and  $91^\circ$  for pDTOc), glass transition temperature ( $99^\circ\text{C}$  for pDTEc and  $53^\circ\text{C}$  for pDTOc), mechanics [pDTEc is brittle (4% elongation at break), while pDTOc is ductile (400% elongation at break)], degradation (pDTEc degrades faster) and biological response [14,27,28]. These differences in properties affect protein adsorption and cell responses such as cell spreading, adhesion and proliferation [27,28].

**Figure 1.** (a) Schematic representation of the combinatorial platform used to fabricate the gradient gas-foamed scaffold libraries. Solutions of pDTEc and pDTOc dispensed from programmed syringe pumps were mixed through a static mixer and deposited onto a trough of sieved  $\text{NH}_4\text{HCO}_3$  crystals ( $250\ \mu\text{m}$  to  $425\ \mu\text{m}$ ); (b) Photograph of a Teflon rig supporting three gas-foamed gradient scaffolds in a large Petri dish. Each gradient is 75 mm long, 8 mm wide and 3 mm deep. A metal wire runs the length of each scaffold gradient enabling them to be suspended in the Petri dish for cell culture experiments.



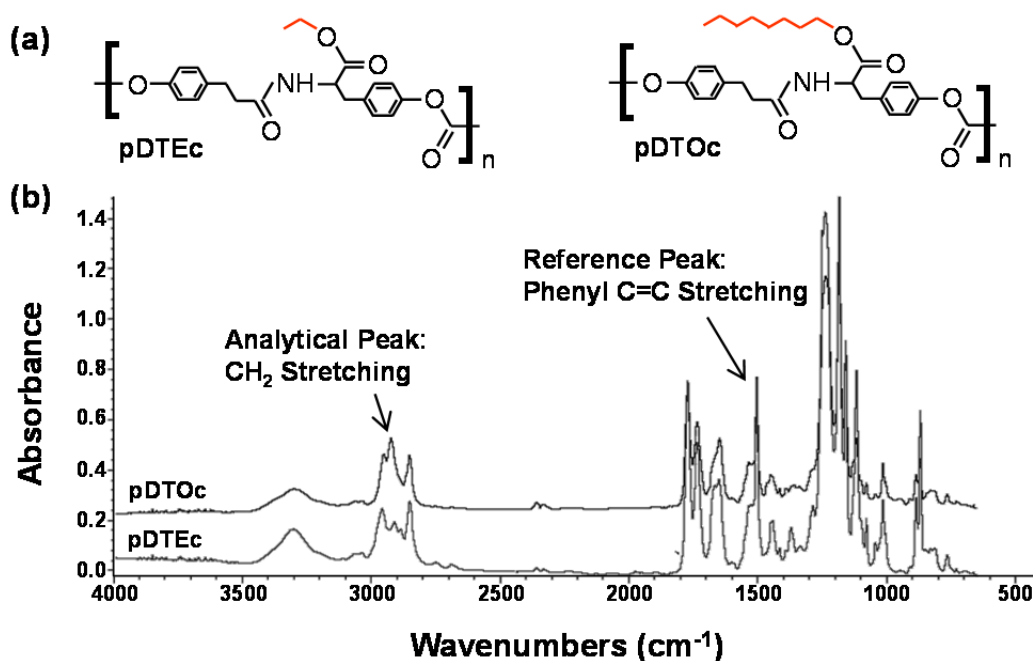
## 2. Experimental Section

### 2.1. Fabrication of Gas-Foamed Gradient Scaffolds

Poly(desaminotyrosyl-tyrosine ethyl ester carbonate) (pDTEc, relative molecular mass 183,000 g/mol) and poly(desaminotyrosyl-tyrosine octyl ester carbonate) (pDTOc, relative molecular

mass 117,000 g/mol) were synthesized as described [27] and solutions of each were made in dioxane (0.1 g/mL). A two-syringe pump system [18,19] was used to fabricate gas-foamed scaffold gradients (Figure 1). Briefly, the pDTEc and pDTOc polymer solutions were loaded into syringes and placed on opposing syringe pumps. pDTEc solution (1 mL) was loaded on the left syringe pump and 2.5 mL of pDTOc solution was loaded on the right pump. The pumps were programmed for a run of 72 s such that the flow rate of the left pump (pDTEc) decreased linearly from 0.5 mL/min to zero while the flow rate of the right pump (pDTOc) increased linearly from zero to 0.5 mL/min. The two solution streams were mixed using a stainless steel static mixer (internal diameter 3.3 mm; catalog # EW-04669-54, Cole-Parmer) which mixes the polymer solutions by cutting and folding them as they flow through a series of helices. This process created effluent at a constant rate of 0.5 mL/min which changed linearly in composition from pDTEc to pDTOc as it eluted from the static mixer.

**Figure 2.** (a) Chemical structure of poly(desaminotyrosyl-tyrosine ethyl ester carbonate) (pDTEc) and poly(desaminotyrosyl-tyrosine octyl ester carbonate) (pDTOc); (b) FTIR spectra for pDTEc and pDTOc after baseline deduction and normalization to maximum absorbance.



Note: Peaks at 2,927 cm<sup>-1</sup> and 1,508 cm<sup>-1</sup> were chosen as the analytical and reference peak, respectively, for quantification.

The effluent was deposited into a rectangular Teflon trough (75 mm long, 8 mm wide, 6 mm deep) containing 3 g of sieved ammonium bicarbonate (NH<sub>4</sub>HCO<sub>3</sub>, 250 μm to 425 μm). A 21 gauge orthodontic wire ran lengthwise along the center of the trough at a height of 2 mm from the bottom of the trough. The wire was designed as a “handle” for mounting the scaffolds and for picking them up. A third syringe pump was fit with a flat stage and used to translate the NH<sub>4</sub>HCO<sub>3</sub> trough at a rate of 3.75 cm/min while the polymers solutions were deposited to create the gradient in deposition. After deposition, gradients were air dried for 30 min in a chemical hood, and then submerged in liquid nitrogen to freeze them. Frozen gradients were placed in a freeze-dryer overnight to remove residual

solvent. Freezedried gradients were removed from the Teflon troughs and placed in warm deionized water (37 °C) for 3 h for gas-foaming of the  $\text{NH}_4\text{HCO}_3$  to create pores. Gradient scaffolds were further leached 3 d in deionized water, air dried and stored in a desiccator. A total of six gradient scaffolds were prepared for this study (three for SEM and three for FTIR).

## 2.2. Characterization of Gradient Scaffolds

For characterization, gradient scaffolds were cut perpendicular to their long axis into seven equal segments (approximately 1.1 cm length per segment) using a scalpel. For scanning electron microscopy (SEM), scaffold segments were sputter-coated with gold and imaged (15 kV, Hitachi S-4700-II FE-SEM). To characterize the pore structure along the gradient, the diameter of the pores was measured in SEM images for segments 1, 4 and 7. For each segment, three SEM images were analyzed and 24 pores were sized for each segment. Scaffold segment compositions were determined by FTIR spectroscopy (NEXUS 670 FTIR spectrophotometer, Nicolet, Thermo Electron). Scaffold segments were individually dissolved in 0.1 mL dioxane and transferred onto KBr discs to record the FTIR spectra (compilation of 64 scans from  $650\text{ cm}^{-1}$  to  $4,000\text{ cm}^{-1}$ , resolution of  $4\text{ cm}^{-1}$ ). Analysis was performed with OMNIC (Version 7.2, Thermo Electron, Chicago, IL, USA). A series of solutions of known composition were prepared by mixing different ratios of pDTEc and pDTOc to prepare an FTIR calibration plot. A linear fit to the calibration plot was used to determine the composition of the unknowns. The porosity of segments 1 and 7 (pDTE-rich and pDTEO-rich, respectively) from the scaffold gradients was determined as described previously [19] using the following formula:  $\text{porosity} = 1 - [(m/d)/v]$ , where  $m$  is the mass of the scaffold,  $d$  is polymer density ( $1.2\text{ g/cm}^3$  for both pDTEc and pDTEO [5]), and  $v$  is the volume of the scaffold.

## 3. Results

A two-syringe pump approach (Figure 1) for fabricating salt-leached scaffold gradients was adapted herein to fabricate gas-foamed scaffold gradients. To demonstrate the approach, two different polymers, pDTEc and pDTEO, were used (Figure 2) to fabricate the gas-foamed scaffold libraries. Three pDTEc/pDTEO gas-foamed scaffold gradients made by the 2-syringe pump approach are shown in Figure 1b. Each gradient was 75 mm long, 8 mm wide and 3 mm deep. The scaffold gradients were mounted in a Teflon rig in a large petri dish. The wires that ran the length of the gradients are visible at the ends of the gradient and were used to suspend the scaffolds in the dish so that they could be used for cell culture experiments.

FTIR was used to characterize the scaffold gradients to map composition. Control spectra for pure pDTEc and pDTEO are presented in Figure 2b. Absorbance at  $1,508\text{ cm}^{-1}$  was chosen as the reference peak (phenyl ring (C=C) stretching) [29] since the phenyl ring structure is the same for pDTEc and pDTEO. Absorbance at  $2,927\text{ cm}^{-1}$  was chosen as the analytical peak ( $\text{CH}_2$  stretching) [30] since the respective ethyl and the octyl side groups in pDTEc and pDTEO are different. An FTIR calibration curve was constructed using known blends of the two polymers (Figure 3a) so that the composition of the gradient scaffold could be assessed. Gradient scaffolds were cut into seven segments and assessed for pDTEc/pDTEO composition using the FTIR calibration plot. The mean composition of 3 gradient scaffolds ranged from 17% pDTEO at the pDTEc-rich end to 84% pDTEO at the pDTEO-rich end

(Figure 3b). The average standard deviation of the mean pDTEc composition for the 7 segments of the 3 gas-foamed gradients was 6%. Previously, salt-leached scaffold gradients were fabricated and they had average standard deviations of the mean composition of 5% for Sudan IV red dye gradients [19] and 14% for gradients of amorphous calcium phosphate nanoparticles [18]. Thus, these results demonstrate that the two-syringe pump gas-foamed scaffold gradient fabrication method yields repeatable gradients that is comparable to previous gradient methodologies. The morphology of the scaffold gradients was assessed by SEM (Figure 4), which revealed a highly interconnected pore structure. The diameter of the pores were measured to be  $(0.21 \pm 0.06)$  mm,  $(0.23 \pm 0.06)$  mm and  $(0.24 \pm 0.06)$  mm for segments 1, 4 and 7 (mean  $\pm$  S.D.,  $n = 24$ ), respectively, and the differences were not statistically significant ( $p > 0.05$ ). The porosity at the pDTEc-rich (segment 1) and pDTEc-poor (segment 7) ends of the gradients was measured to be  $(97.9 \pm 3.0)\%$  ( $n = 5$ ) and  $(96.9 \pm 3.6)\%$  ( $n = 6$ ), respectively, and these values also were not statistically different ( $p > 0.05$ ). These results show that the scaffold structure was similar across the gradients and that the change in pDTEc/pDTEc composition in the gradients did not affect pore structure.

**Figure 3.** (a) Calibration plot of FTIR peak absorbance ratios ( $2,927\text{ cm}^{-1}$ :  $1,508\text{ cm}^{-1}$ ) for known control mixtures of pDTEc and pDTEc. The dashed line is a linear fit ( $y = 0.0064x + 0.0596$ ) with Pearson correlation coefficient (R) of 0.99; (b) Plot of pDTEc content in the different segments of the gradient scaffolds (error bars are standard deviation,  $n = 3$ ). The slope of the linear fit (dashed line) is significantly greater than zero (t-test,  $p < 0.05$ ) with a Pearson correlation coefficient (R) of 0.98.

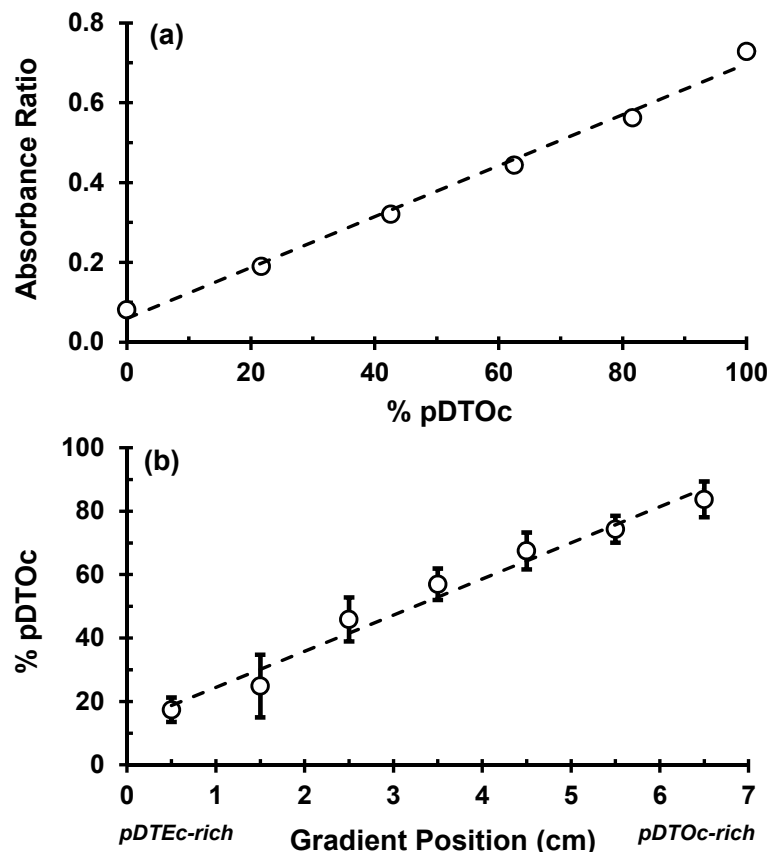
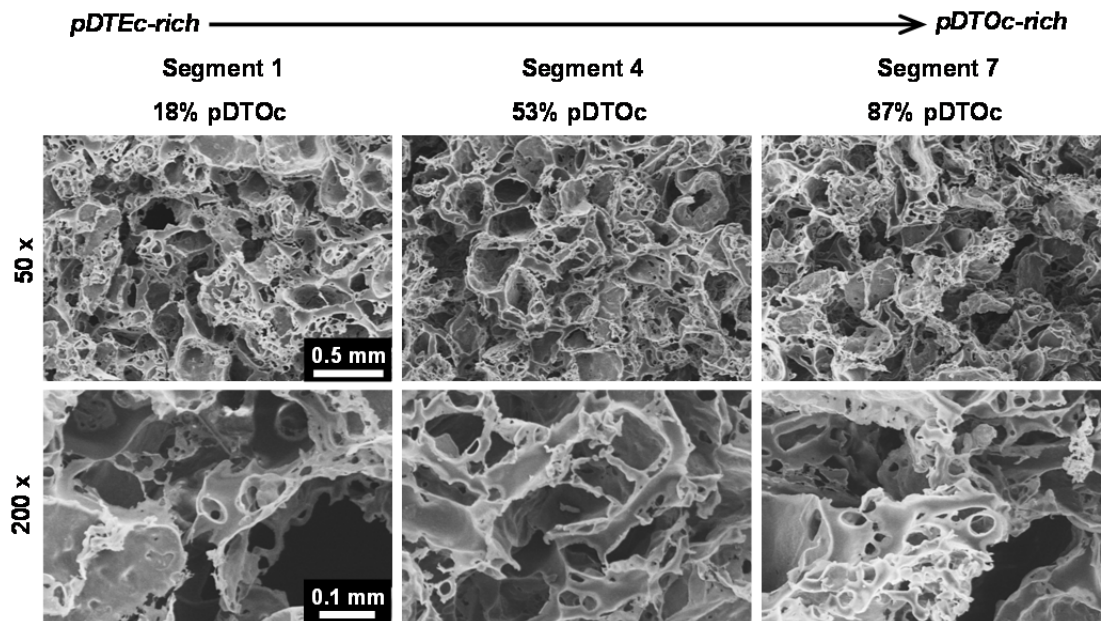


**Figure 4.** Scanning electron micrographs of the 3D gas-foamed gradient scaffolds at 50× (top row) and 200× (bottom row) magnification showing the interconnected porous structure.



#### 4. Discussion

The current work establishes a two-syringe pump approach for fabricating gas-foamed scaffold gradients that can be used for combinatorial screening of cell-material interactions in 3D. Methods for salt-leached scaffolds [14,18,19], hydrogels [15,17], nanofiber scaffolds [31–34] and gas-foamed scaffolds (current work) have been described for combinatorial screening in 3D. In the salt-leaching method, the sodium chloride crystals serve as a porogen which is leached by dissolution in water. The final scaffold pores match the size and shape (cuboidal) of the starting salt crystals [10]. When gas-foaming, the ammonium bicarbonate serves as both a porogen and as a source of gas bubbles. During ammonium bicarbonate dissolution, ammonia and carbon dioxide gases are generated from the reaction with water. The release of gas bubbles provides additional interconnections between pores. The gas bubbles must squeeze out of the scaffold which changes the final pore morphology, making the pores smaller in size than the starting crystals and irregular in shape. In Kumar *et al.* [10] salt-leached and gas-foamed scaffolds were made from the same polymer (PCL) using the same sieve sizes for the NaCl and ammonium bicarbonate (250  $\mu\text{m}$  to 425  $\mu\text{m}$ ), respectively. SEMs of these scaffolds showed that: (1) the salt-leached scaffolds had larger pores than the gas-foamed scaffolds; (2) the gas-foamed pores were more irregularly shaped than the cuboidal salt-leached pores; (3) the gas-foamed had more overall pores than the salt-leached (due to gas bubble release). The gas-foamed gradients in the current work (Figure 4) also had had irregularly shaped pores that were smaller in size (210  $\mu\text{m}$  to 240  $\mu\text{m}$ ) than the starting ammonium bicarbonate crystals (250  $\mu\text{m}$  to 425  $\mu\text{m}$ ).

Scaffold gradients are useful for systematically screening cell response to scaffold properties because all scaffold samples can be contained in a single culture dish to reduce well-to-well variability [18]. Scaffold gradients can also be used for engineering graded tissues [35]. For instance, ligaments and tendons join soft and hard tissues and contain gradients from cartilage to bone [36]. Scaffolds containing gradients can be used to spatially control cell function to generate tissue gradients

to restore native hierarchical structure [37,38]. Herein, gas-foamed scaffolds were fabricated with a polymer composition gradient. However, the method is adaptable to any components that can be processed via liquid mixing including gradients of nanoparticles, calcium phosphate composites, encapsulated growth factors, peptide-functionalized polymers or vectors (virus, plasmid).

## 5. Conclusions

A two-syringe pump method for fabricating gas-foamed scaffold gradients has been developed. Gradients in scaffold polymer composition were fabricated using two polymers with different properties, pDTEc and pDTOc. The new method yielded gas-foamed scaffolds with repeatable gradients in polymer composition and a consistent pore structure. This new approach for fabricating gas-foamed scaffold gradients can be used for combinatorial screening of cell-material interactions in 3D.

## Acknowledgments

K.C. was supported by a postdoctoral fellowship from NIH-NIBIB/NIST NRC. The standard deviation is the same as the “combined standard uncertainty of the mean” for the purposes of this work. The content is solely the responsibility of the authors and does not necessarily represent the official views of NIST. This article, a contribution of NIST, is not subject to USA copyright. Certain equipment and instruments or materials are identified in the paper to adequately specify the experimental details. Such identification does not imply recommendation by NIST, nor does it imply the materials are necessarily the best available for the purpose.

## References

1. Simon, C.G.; Yang, Y.; Thomas, V.; Dorsey, S.M.; Morgan, A.W. Cell interactions with biomaterials gradients and arrays. *Comb. Chem. High T. Scr.* **2009**, *12*, 544–553.
2. Simon, C.G., Jr; Lin-Gibson, S. Combinatorial and high-throughput screening of biomaterials. *Adv. Mater.* **2011**, *23*, 369–387.
3. Meredith, J.C.; Sormana, J.L.; Keselowsky, B.G.; Garcia, A.J.; Tona, A.; Karim, A.; Amis, E.J. Combinatorial characterization of cell interactions with polymer surfaces. *J. Biomed. Mater. Res.* **2003**, *66A*, 483–490.
4. Lin, N.J.; Lin-Gibson, S. Osteoblast response to dimethacrylate composites varying in composition, conversion and roughness using a combinatorial approach. *Biomaterials* **2009**, *30*, 4480–4487.
5. Yang, J.; Rose, F.R.A.J.; Gadegaard, N.; Alexander, M.R. A high-throughput assay of cell-surface interactions using topographical and chemical gradients. *Adv. Mater.* **2009**, *21*, 300–304.
6. Mei, Y.; Saha, K.; Bogatyrev, S.R.; Yang, J.; Hook, A.L.; Kalcioglu, Z.I.; Cho, S.W.; Mitalipova, M.; Pyzocha, N.; Rojas, F.; *et al.* Combinatorial development of biomaterials for clonal growth of human pluripotent stem cells. *Nat. Mater.* **2010**, *9*, 768–778.
7. Unadkat, H.V.; Hulsman, M.; Cornelissen, K.; Papenburg, B.J.; Truckenmuller, R.K.; Post, G.F.; Uetz, M.; Reinders, M.J.; Stamatialis, D.; van Blitterswijk C.A.; *et al.* An algorithm-based topographical biomaterials library to instruct cell fate. *Proc. Natl. Acad. Sci. USA* **2011**, *108*, 16565–16570.



8. Place, E.S.; Evans, N.D.; Stevens, M.M. Complexity in biomaterials for tissue engineering. *Nat. Mater.* **2009**, *8*, 457–470.
9. Dalby, M.J.; Gadegaard, N.; Tare, R.; Andar, A.; Riehle, M.O.; Herzyk, P.; Wilkinson, C.D.; Oreffo, R.O. The control of human mesenchymal cell differentiation using nanoscale symmetry and disorder. *Nat. Mater.* **2007**, *6*, 997–1003.
10. Kumar, G.; Tison, C.K.; Chatterjee, K.; Pine, P.S.; McDaniel, J.H.; Salit, M.L.; Young, M.F.; Simon, C.G., Jr. The determination of stem cell fate by 3D scaffold structures through the control of cell shape. *Biomaterials* **2011**, *32*, 9188–9196.
11. Hall, H.G.; Farson, D.A.; Bissell, M.J. lumen formation by epithelial-cell lines in response to collagen overlay—A morphogenetic model in culture. *Proc. Natl. Acad. Sci. USA* **1982**, *79*, 4672–4676.
12. Abbott, A. Cell culture: Biology's new dimension. *Nature* **2003**, *424*, 870–872.
13. Griffith, L.G.; Swartz, M.A. Capturing complex 3D tissue physiology *in vitro*. *Nat. Rev. Mol. Cell Biol.* **2006**, *7*, 211–224.
14. Yang, Y.; Bolikal, D.; Becker, M.L.; Kohn, J.; Zeiger, D.N.; Simon, C.G., Jr. Combinatorial polymer scaffold libraries for screening cell-biomaterial interactions in 3D. *Adv. Mater.* **2008**, *20*, 2037–2043.
15. Chatterjee, K.; Lin-Gibson, S.; Wallace, W.E.; Parekh, S.H.; Lee, Y.J.; Cicerone, M.T.; Young, M.F.; Simon, C.G., Jr. The effect of 3D hydrogel scaffold modulus on osteoblast differentiation and mineralization revealed by combinatorial screening. *Biomaterials* **2010**, *31*, 5051–5062.
16. Chatterjee, K.; Young, M.F.; Simon, C.G., Jr. Fabricating gradient hydrogel scaffolds for 3D cell culture. *Comb. Chem. High T. Scr.* **2010**, *14*, 227–236.
17. Yang, F.; Cho, S.W.; Son, S.M.; Hudson, S.P.; Bogatyrev, S.; Keung, L.; Kohane, D.S.; Langer, R.; Anderson, D.G. Combinatorial extracellular matrices for human embryonic stem cell differentiation in 3D. *Biomacromolecules* **2010**, *11*, 1909–1914.
18. Chatterjee, K.; Sun, L.; Chow, L.C.; Young, M.F.; Simon, C.G., Jr. Combinatorial screening of osteoblast response to 3D calcium phosphate/poly(epsilon-caprolactone) scaffolds using gradients and arrays. *Biomaterials* **2011**, *32*, 1361–1369.
19. Simon, Jr., C.G.; Stephens, J.S.; Dorsey, S.M.; Becker, M.L. Fabrication of combinatorial polymer scaffold libraries. *Rev. Sci. Instrum.* **2007**, *78*, 0722071-072207.
20. Yang, Y.; Dorsey, S.M.; Becker, M.L.; Lin-Gibson, S.; Schumacher, G.E.; Flaim, G.A.; Kohn, J.C.; Simon, C.G., Jr. X-ray imaging optimization of 3D tissue engineering scaffolds via combinatorial fabrication methods. *Biomaterials* **2008**, *29*, 1901–1911.
21. Harris, L.D.; Kim, B.S.; Mooney, D.J. Open pore biodegradable matrices formed with gas foaming. *J. Biomed. Mater. Res.* **1998**, *42*, 396–402.
22. Nam, Y.S.; Yoon, J.J.; Park, T.G. A novel fabrication method of macroporous biodegradable polymer scaffolds using gas foaming salt as a porogen additive. *J. Biomed. Mater. Res.* **2000**, *53*, 1–7.
23. Shea, L.D.; Wang, D.; Franceschi, R.T.; Mooney, D.J. Engineered bone development from a pre-osteoblast cell line on three-dimensional scaffolds. *Tiss. Eng.* **2000**, *6*, 605–617.

24. Salerno, A.; Zeppetelli, S.; Di, M.E.; Iannace, S.; Netti, P.A. Processing/structure/property relationship of multi-scaled PCL and PCL-HA composite scaffolds prepared via gas foaming and NaCl reverse templating. *Biotechnol. Bioeng.* **2011**, *108*, 963–976.
25. Kohn, J. Implants: The biodegradable future. *Med. Device Dev.* **2006**, *February*, 35–36.
26. Kim, J.; Magno, M.H.; Alvarez, P.; Darr, A.; Kohn, J.; Hollinger, J.O. Osteogenic differentiation of pre-osteoblasts on biomimetic tyrosine-derived polycarbonate scaffolds. *Biomacromolecules* **2011**, *12*, 3520–3527.
27. Ertel, S.I.; Kohn, J. Evaluation of a series of tyrosine-derived polycarbonates as degradable biomaterials. *J. Biomed. Mater. Res.* **1994**, *28*, 919–930.
28. Bailey, L.O.; Becker, M.L.; Stephens, J.S.; Gallant, N.D.; Mahoney, C.M.; Washburn, N.R.; Rege, A.; Kohn, J.; Amis, E.J. Cellular response to phase-separated blends of tyrosine-derived polycarbonates. *J. Biomed. Mater. Res. A.* **2006**, *76*, 491–502.
29. Babu, K.S.; Srinivas P.V.; Praveen, B.; Kishore K.H.; Murty, U.S.; Rao J.M. Antimicrobial constituents from the rhizomes of *Rheum emodi*. *Phytochemistry* **2003**, *62*, 203–207.
30. Kesters, E.; de Kok, M.M.; Carleer, R.A.A.; Czech, J.H.P.B.; Adriaensens, P.J.; Gelan, J.M.; Vanderzande, D.J. The thermal conversion reaction of sulphonyl substituted poly( para-xylylene): Evidence for the formation of PPV structures. *Polymer* **2002**, *43*, 5749–5755.
31. Li, X.R.; Xie, J.W.; Lipner, J.; Yuan, X.Y.; Thomopoulos, S.; Xia, Y.N. Nanofiber scaffolds with gradations in mineral content for mimicking the tendon-to-bone insertion site. *Nano Lett.* **2009**, *9*, 2763–2768.
32. Valmikinathan, C.M.; Wang, J.P.; Smiriglio, S.; Golwala, N.G.; Yu, X.J. Magnetically induced protein gradients on electrospun nanofibers. *Comb. Chem. High T. Scr.* **2009**, *12*, 656–663.
33. Samavedi, S.; Olsen, H.C.; Guelcher, S.A.; Goldstein, A.S.; Whittington, A.R. Fabrication of a model continuously graded co-electrospun mesh for regeneration of the ligament-bone interface. *Acta Biomater.* **2011**, *7*, 4131–4138.
34. Ramalingam, M.; Young, M.F.; Thomas, V.; Sun, L.; Chow, L.C.; Tison, C.K.; Chatterjee, K.; Miles, W.C.; Simon Jr., C.G. Nanofiber scaffold gradients for interfacial tissue engineering. *J. Biomat. Appl.* **2012**, in press.
35. Dormer, N.H.; Berkland, C.J.; Detamore, M.S. Emerging techniques in stratified designs and continuous gradients for tissue engineering of interfaces. *Ann. Biomed. Eng.* **2010**, *38*, 2121–2141.
36. Moffat, K.L.; Sun, W.H.; Pena, P.E.; Chahine, N.O.; Doty, S.B.; Ateshian, G.A.; Hung, C.T.; Lu, H.H. Characterization of the structure-function relationship at the ligament-to-bone interface. *Proc. Natl. Acad. Sci. USA* **2008**, *105*, 7947–7952.
37. Phillips, J.E.; Burns, K.L.; Le Doux, J.M.; Guldborg, R.E.; Garcia, A.J. Engineering graded tissue interfaces. *Proc. Natl. Acad. Sci. USA* **2008**, *105*, 12170–12175.
38. Harley, B.A.; Lynn, A.K.; Wissner-Gross, Z.; Bonfield, W.; Yannas, I.V.; Gibson, L.J. Design of a multiphase osteochondral scaffold III: Fabrication of layered scaffolds with continuous interfaces. *J. Biomed. Mater. Res. A* **2010**, *92*, 1078–1093.